

COST-EFFICIENT METHODS OF DERIVING SLOPE INFORMATION FOR ROAD SEGMENTS IN DRIVER-ASSISTANCE APPLICATIONS

V. Horváth¹*, A. Barsi¹

¹ Dept. Photogrammetry and Geoinformatics, Budapest University of Technology and Economics, Hungary -
(horvath.viktor.gyozo, barsi.arpad)@emk.bme.hu

WG Navigation, Guidance and Control of Autonomous Vehicles

KEY WORDS: GIS, slope maps, ADAS, crowdsourcing

ABSTRACT:

An advanced driver-assistance system (ADAS) is any of a group of technologies that assist drivers in driving and parking functions. Through a safe human-machine interface, ADAS increase car and road safety. These Advanced driver-assistance systems rely on special maps with extended geometry and attribute information. This extra information includes slope, curvature, and speed limit. ADAS-enabled maps are usually rather expensive in the industry. This paper is focused on finding cost-efficient alternatives for generating the slope aspect of ADAS maps. Slope and height information is not only used in ADAS but is a critical aspect of calculating electronic vehicle (EV) ranges, and truck fuel-efficiency calculations as well. ADAS slope information usually requires high-accuracy surveys. This paper researches the possible generation of slope information for road segments with the use of digital elevation models (DEM) or crowdsourcing with low-cost sensors and Kalman filtering. The first approach is based on globally available DEMs with interpolation and filtering with road geometry. DEMs have variable accuracy depending on the type of technology used in producing them. Such technologies include photogrammetry, aerial and terrestrial laser scanning (ALS, TLS), or aerial or space radar measurements. The other method is by using low-cost GPS and IMU sensors for generating altitude profiles. These produced altitude profiles are compared with a profile generated from a high-accuracy survey using large-resolution DEMs produced by aerial photogrammetry or aerial laser scanning. This paper proposes metrics with which these datasets can be compared, one is using the height differences, and the other compares the slope values at discrete common points. In the conclusion, the paper tries to find use cases for the low-accuracy data.

1. INTRODUCTION

Driver assistance systems are designed to reduce accidents and collisions. They make driving safer and can potentially lower insurance premiums.

In the beginning, vehicles were driven exclusively by humans. Then, mainly in order to make driving safer, various systems began to be developed, which provided the driver with helpful information about the state of the vehicle and its environment (DIS - Driver Information Systems). For example, with a camera mounted on a vehicle, the vehicle also detects the speed indication on traffic signs and then shows the speed limit extracted from the image to the driver so that he can always see the current speed limit.

The next step in development is the appearance of driver assistance systems (DAS - Driver Assistance Systems). Their primary purpose is to make traffic safer. The vast majority of emergency situations involve sudden braking; for example the anti-lock braking system (ABS - Anti-lock Braking System) helps with this. ABS prevents the wheel from slipping, so controllability is preserved longer than a vehicle that is slipping. This development can also be observed in the case of cruise control (CC - Cruise Control). In its early version, the vehicle drove at the input speed, sparing the driver's feet from continuous pedal pressure on longer road sections, which typically apply to highways. Then, with the advent of adaptive cruise control (ACC - Adaptive Cruise Control), the vehicle already monitors the other vehicle in front of it and adjusts the set speed to that of the vehicle in front.

Adaptive cruise control already belongs to advanced driver support systems (ADAS - Advanced Driver Assistance Systems). These developments typically appeared later than those listed above, and they make better use of the data obtained with the vehicle's sensors. When driving the vehicle, cross-directional movement can also be dangerous. The lane departure warning system (LDW - Lane Departure Warning), for example, monitors the road with a camera, and if the vehicle leaves its lane without using the turn signal, the vehicle warns the driver, typically by vibrating the steering wheel. In addition to the warning, the lane-keeping assistant (LKAS - Lane Keeping Assist System) also carefully steers the vehicle back into its own lane. The Lane Change Assist (LCA - Lane Change Assist) not only checks the vehicle in the blind spot but also switches the vehicle to the lane next to it if there is none. [Barsi et al 2020]

ADAS is an alternative term for passive and active safety systems designed to remove the human error component from the operation of many types of vehicles. ADAS systems use advanced technologies to assist the driver while driving, thereby improving driver performance. ADAS uses a combination of sensor technologies to perceive the world around the vehicle and then either provide information to the driver or take action when necessary.

Due to vehicle dynamics, shifting problems on hilly roads are essential. With the road information provided by a high-resolution (HD) digital map, frequent shifting can be eliminated, and improved dynamic performance on uphill roads can be achieved so that unnecessary upshifts can be avoided, and engine traction resistance can be used to assist the braking system when a vehicle is traveling downhill. Fuel consumption

* Corresponding author

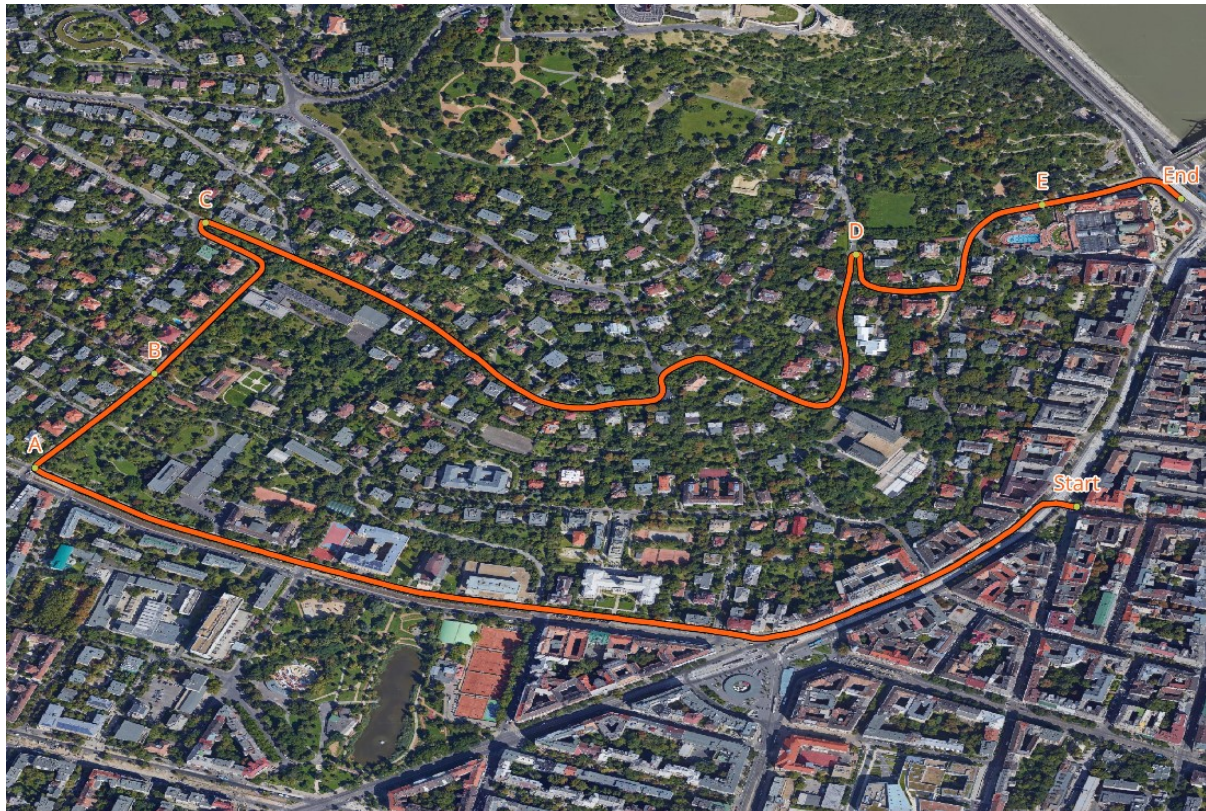


Figure 1. The study area with the investigated road profile in red

and maintenance costs can also be significantly reduced. A possible new shift strategy offers a reliable and effective solution to improve vehicle driving performance in hilly environments. [Meng and Jin, 2018]

It is trivial to note that road gradients (slopes) critically affect the electricity consumption of electric vehicles (EVs). A significantly better model of electricity consumption can be achieved by categorizing slopes and assigning a percentage of the trip distance to each category. [Liu et al, 2017]

2. DATA SETS AND METHODOLOGY

The study area is located in the center of Budapest on the side of Gellért Hill. There are significant differences in altitude on the road: the range of the height is 61.55 meter. The length of the surveyed section is 3200 m. A value was assigned to the section every 0.75 meters. The ground truth Digital Surface Model (DSM) was generated using large resolution aerial photogrammetry by the Lechner Knowledge Centre (Fig. 1). Unfortunately, the obtained DSM contains noises, supposedly because of the effect of the vegetation. The investigated trajectory was marked in five significant places labelled from A to E.

The DSM had to be assembled from tiles and then sampled along the road section under study. The QGIS (3.32) software and its qprof addon were used for this purpose. qProf is a plugin for the generation of topographic and geological profiles. Topography can be extracted from DEM or GPX files.

The data were further processed in MathWorks Matlab R2023a environment. The DSM was georeferenced in the Hungarian EO/HD72 (EPSG: 23700) coordinate reference system (CRS). All the other data used were transformed into the same CRS using the default projection between the two systems used by QGIS. The DSM was in Float32 (single-precision floating-point) geoTIFF format. It had a spatial resolution of 8 centimeters, and a coverage of 1400 by 1100 meters.

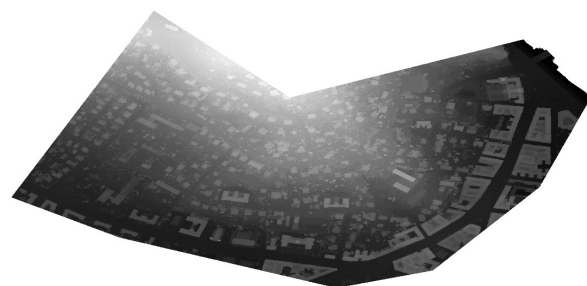


Figure 2. The ground truth digital surface model obtained from photogrammetric image evaluation.

A Digital Elevation Model (DEM) is a representation of the bare ground (bare earth) topographic surface of the Earth excluding trees, buildings, and any other surface objects. DEMs are created from a variety of sources. The Shuttle Radar Topography Mission (SRTM) is an international research effort that obtained digital elevation models on a near-global scale

from 56°S to 60°N, to generate the most complete high-resolution digital topographic database of Earth prior to the release of the ASTER GDEM in 2009 [Rabus et al, 2003]. In the case of SRTM as the name suggests altitudes are obtained by measuring distances with RADAR. In our studies an SRTM tile with a spatial resolution of 30 meters was used.

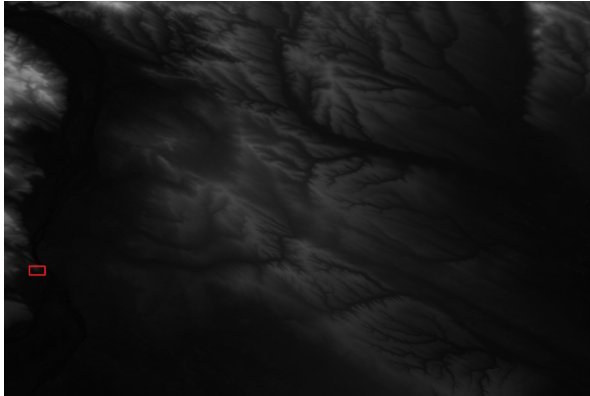


Figure 3. SRTM Digital Elevation Model with the study area marked by red rectangle.

The Advanced Spaceborne Thermal Emission and Reflection Radiometer (ASTER) is a Japanese remote sensing instrument onboard the Terra satellite launched by NASA in 1999 [Fujisada et al, 2006]. It has been collecting data since February 2000. On 29 June 2009, the Global Digital Elevation Model (GDEM) was released. A joint operation between NASA and Japan's Ministry of Economy, Trade and Industry (METI), the Global Digital Elevation Model is the most complete mapping of the earth ever made, covering 99% of its surface. The spatial resolution in the case of this DEM is also 30 meters, but the altitudes obtained are produced via photogrammetry.

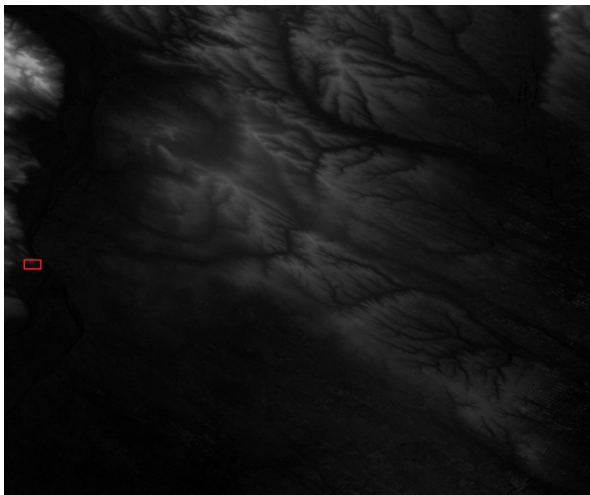


Figure 4. Aster GDEM model for the pilot area (red rectangle).

Android phones can be used to collect data quickly in a crowdsourced model. The measured and Kalman filtered positions are accessed by Android's Location API [https://developer.android.com/training/location]. Most Android devices allow to determine the current geolocation. This can be done via a GPS (Global Positioning System) module, via cell tower triangulation and via wi-fi networks. LocationProvider (a

development class in Android) provides the best positioning available at the given moment via implementation of sensor fusion using Kalman Filtering.

AndroSensor is an application for smartphones running an Android OS; it supports all the sensors an Android device can have. It can log the data from the following sensors in a CSV format.

- location, location provider, accuracy, altitude, speed and GPS NMEA data.
- accelerometer readings, (incl. linear acceleration and gravity sensors)
- gyroscope readings,
- light sensor value,
- ambient magnetic field values,
- device orientation
- pressure sensor (barometer)
- relative humidity sensor
- proximity sensor readings
- temperature readings
- battery status, voltage, temperature and health
- sound level meter (decibel).

Thanks to the option to log the data in a CSV format processing is easier.

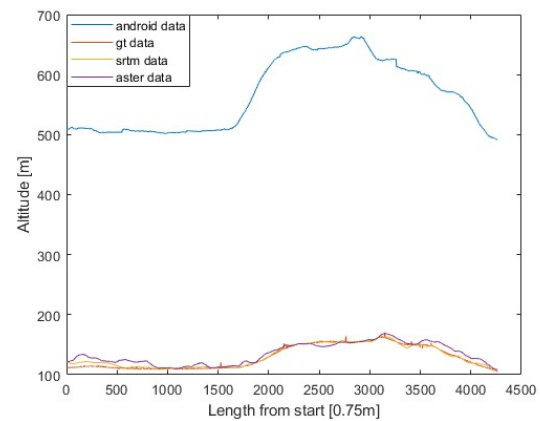


Figure 5. Elevation information along the trajectory.

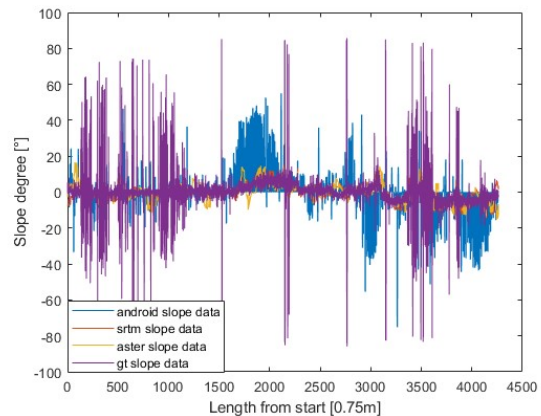


Figure 6. Slope values in degrees derived from the elevation data sources.

Fig. 5 presents the elevation profiles obtained from all available data sets. SRTM, Aster and photogrammetry-based height data have quite good fit, while Android observations seems to show similar tendency but having simultaneously a scaling effect. Based on the elevation data, the slope values are easily to be derived. Slope has higher relevance in the practical application; the previously mentioned hill-assistant consider slope information. Unfortunately, the derived values have relatively high standard deviation (Table 1). The reason can be the improper vegetation removal during the creation of the elevation model.

Slope in degrees	Median	Mean	Standard deviation
Android	0.1514	0.0268	18.1169
Aster	-0.0973	-0.0227	13.4642
SRTM	-0.3075	0.0170	12.9940

Table 1. Statistics of the slope for Android, Aster and SRTM

3. RESULTS

The study compares the derived slopes from the raw measurement, and also proposes a way to calculate more reliable slope data from each source. The first preprocessing phase was the removal of the average altitude values from all profiles. Then the proposed method is an automated outlier removal with a 50 unit long moving median, then a smoothing using a locally weighted scatterplot smoothing (LOWESS). The obtained elevation profiles can be seen in Fig. 7.

Starting point and Point A has approximately the same elevation, but after the right turn the trajectory starts running uphill. Point B has been marked as an intermediate altitude point between A and C. The trajectory after point C has some increase and ends at point D. The route is decreasing thereafter as point E has a clear slower height.

The corresponding slope charts are visualized similarly; Fig. 8 presents the derived slope values for the applied data sources. Slope values are interpreted in degrees. The chart shows the effect of the mean removal and the smoothing.

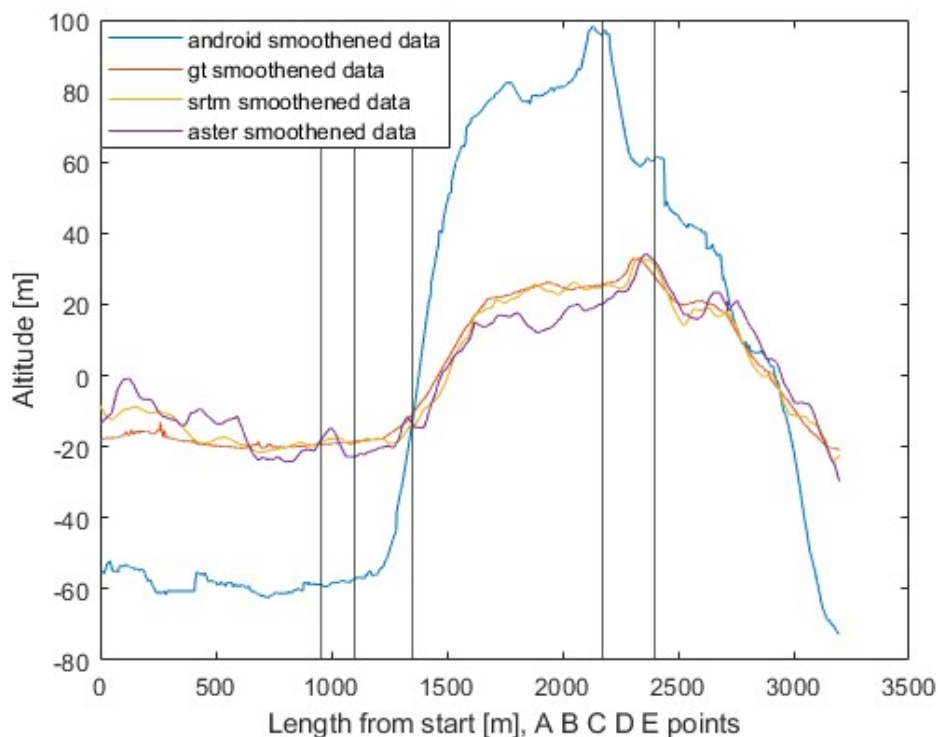


Figure 7. Elevation information along the trajectory after outlier removal and smoothing. Vertical lines represent the trajectory points A to E, respectively

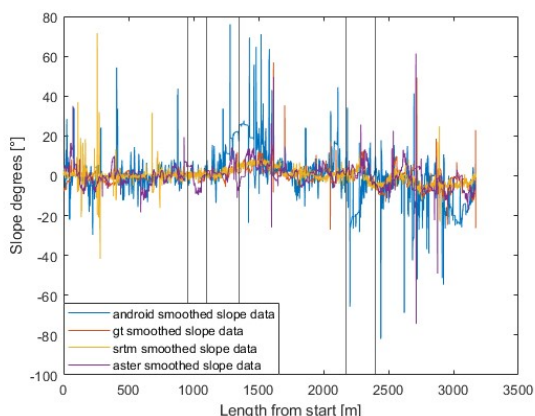


Figure 8. Slope values in degrees derived from the elevation data sources after outlier removal and smoothing. Vertical lines represent the trajectory points A to E, respectively

The data set preparation with average removal and smoothing is clearly visible in the derived statistics. Compared to Table 1, the newly obtained statistics (Table 2) shows definitely fewer standard deviations in all data sets. The means and medians are the same in dm range.

Slope in degrees	Median	Mean	Standard deviation
Android	0.1970	-0.1437	10.8534
Aster	-0.1732	-0.11667	6.1427
SRTM	-0.2837	-0.22856	4.7929

Table 2. Statistics of the slope for Android, Aster and SRTM after outlier removal and smoothing.

4. CONCLUSION

In our tests, we compared SRTM and ASTER-based digital elevation models derived by photogrammetry with on-board Android measurements. We found that the height models show a high degree of similarity, i.e. no significant difference can be observed between the available height databases. At the same time, due to the large scale, the local effect of the vegetation becomes more apparent: a significant height variance can be observed in the data due to the trees.

The Androsensor measurements run on a smart device placed on the vehicle deck show a similar behavior as the data in the databases, however, in addition to a different regular shift (different height average), they also differ in a certain scale factor. In the operation of the vehicle assistants, the slope data is of paramount importance, however, based on the tests, it is recommended to normalize and smooth the slope values derived based on the height.

ACKNOWLEDGEMENT

The research reported in this paper and carried out at the Budapest University of Technology and Economics has been supported by the National Research Development and Innovation Fund (TKP2020 Institution Excellence Subprogram, Grant No. BME-IE-MIFM) based on the charter of bolster issued by the National Research Development and Innovation

Office under the auspices of the Ministry for Innovation and Technology.

The project has been supported by the European Union, co-financed by the European Social Fund. EFOP-3.6.3-VEKOP-16-2017-00001.

The authors are grateful to the Lechner Knowledge Center for the topography data provided for the research.

REFERENCES

- Chan, K.L., Qin K., 2017: Biomass burning related pollution and their contributions to the local air quality in Hong Kong. *Int. Arch. Photogramm. Remote Sens. Spatial Inf. Sci.*, XLII-2/W7, 29-36. DOI: doi.org/10.5194/isprs-archives-XLII-2-W7-29-2017.
- Gupta, A., Khare, A., Jin, H., Sadek, A., Su, L., Qiao, C., 2020. Estimation of Road Transverse Slope Using Crowd-Sourced Data from Smartphones, ACM, Proceedings of the 28th International Conference on Advances in Geographic Information Systems
- Ustunel, E., Masazade, E., 2019. Vision based road slope estimation methods using road lines or local features from instant images, IET Intelligent Transport Systems, Vol. 13, No. 10, pp. 1590-1602
- Caroti, G., Piemonte, A., 2010. Measurement of cross-slope of roads: evaluations, algorithms and accuracy analysis, Survey Review, Vol. 42, No. 315, pp. 92—104
- Lu, Y., Karimi, H., 2015. Real-Time Sidewalk Slope Calculation through Integration of GPS Trajectory and Image Data to Assist People with Disabilities in Navigation, ISPRS International Journal of Geo-Information, Vol. 4, No. 2, pp. 741—753
- Matsui, T., Sukanuma, N., 2011. Road Region Extraction with Longitudinal Slope, Transactions of the Japan Society of Mechanical Engineers Series C, Vol. 77, No. 782, pp. 3737—3749
- Sebsadji, Y., Glaser, S., Mammari, S., Dakhllallah, J., 2008. Road slope and vehicle dynamics estimation, American Control Conference
- Ren, Z., 2014. Road Slope Estimation Algorithm and Safety Analysis of Mountainous Road, Journal of Information and Computational Science, Vol. 11, No. 7, pp. 2253—2265
- Jin, H., Ge, A., 2007. On the intelligent slope shift strategy, Proceedings of the Institution of Mechanical Engineers, Part D: Journal of Automobile Engineering, SAGE Publications, Vol. 221, No. 8, pp. 991—999
- Meng, F., Jin, H., 2018. Slope Shift Strategy for Automatic Transmission Vehicles Based on the Road Gradient, International Journal of Automotive Technology, Vol. 19, No. 3, pp. 509—521
- Barsi, Á., Csepinszky, A., Lógó, J.M., Krausz, N., Potó, V., 2020: Map-based support for self-driving, in Hungarian, *Geodézia és Kartográfia*, Vol. 2020, No. 2, pp. 10-15, DOI: doi.org/10.30921/GK.72.2020.2.2
- Meng, F., Jin, H. 2018: Slope Shift Strategy for Automatic Transmission Vehicles Based on the Road Gradient - *Int.J*

Automot. Technol. 19, 509–521, DOI: doi.org/10.1007/s12239-018-0049-5

Liu, K., Yamamoto, T., Morikawa, T. 2017: Impact of road gradient on energy consumption of electric vehicles - *Transportation Research Part D: Transport and Environment*, Vol. 54, 2017, pp. 74-81, ISSN 1361-9209, DOI: doi.org/10.1016/j.trd.2017.05.005.

Suau, A., Staffelbach, G., Todri-Sanialqprof, A. 2023: A gprof-Inspired Quantum Profiler - *ACM Transactions on Quantum Computing*, Vol. 4, No. 1, DOI: doi.org/10.1145/3529398

Rabus, B., Eineder, M., Roth, A., Bamler, R. 2003: The Shuttle Radar Topography Mission. - New Class of Digital Elevation Models Acquired by Spaceborne Radar. *ISPRS Journal of Photogrammetry and Remote Sensing*. Vol. 57, pp. 241-26, DOI: doi.org/10.1016/S0924-2716(02)00124-7.

Fujisada, H., Bailey, G., Glenn, K., Hara, S., Abrams, M. 2006: ASTER DEM performance. *IEEE Transactions on Geoscience and Remote Sensing*, Vol. 43, pp. 2707-2714, DOI: doi.org/10.1109/TGRS.2005.847924.

<https://developer.android.com/training/location>